

# Using weigh-in-motion data to determine bridge dynamic amplification factor

Jan Kalin<sup>1,a</sup>, Aleš Žnidarič<sup>1</sup> and Maja Kreslin<sup>1</sup>

<sup>1</sup>*Slovenian National Building and Civil Engineering Institute, Department of Structures, The Section for Bridges and Other Engineering Structures, Ljubljana, Slovenia.*

**Abstract.** The dynamic component of bridge traffic loading is commonly taken into account with a Dynamic Amplification Factor (DAF) – the ratio between the maximum dynamic and static load effects on a bridge. In the design codes, this factor is generally higher than in reality. While this is fine for new bridges that must account for various risks during their life-time, it imposes unnecessary conservatism into assessment of the existing well defined bridges. Therefore, analysis of existing bridges should apply more realistic DAF values. One way of obtaining them experimentally is by bridge weigh-in-motion (B-WIM) measurements, which use an existing instrumented bridge or culvert to weigh all crossing vehicles at highway speeds. The B-WIM system had been equipped with two methods of obtaining an approximation to the static response of the. The first method uses the sum of influence lines. This method relies on accurate axle identification, the failure of which can have a large influence on the DAF value. The other method uses a pre-determined low-pass filter to remove the dynamic component of the measured signal; however an expert is needed to set the filter parameters. A new approach that tries to eliminate these two drawbacks has been developed. In this approach the parameters for the filter are determined automatically by fitting the filtered response to the sum of the influence lines. The measurement of DAF on a typical bridge site agrees with experiments performed in the ARCHES [1] project: dynamic amplification decreases as static loading increases.

## 1 Introduction

Correct evaluation of the behaviour of highway bridges under heavy traffic loading is extremely important both for the enhancement of design techniques and for the assessment of existing infrastructure. It is widely accepted that shortfalls exist in the determination of the traffic loads which the bridge may be required to support during its expected lifetime, due to inadequate consideration of, amongst other factors, the dynamic interaction between the bridge structure and the heavy vehicles crossing it.

The FP6 ARCHES project [1] went into some detail of the dynamic effects of traffic on bridges. It provided an overview of the current building code recommendations for dynamic allowances and compared those with the simulations and with the measured allowances obtained using bridge weigh-in-motion (B-WIM) measurements on several bridges. One of the more important conclusions was that the design code recommendations are generally conservative with respect to true dynamic allowance values, especially at higher (extreme) traffic loads. For assessing of existing bridges, and in many cases extending their lifetime, it is thus beneficial to apply more accurate methods of estimating dynamic allowances.

The measurements for the ARCHES project were made with the 2<sup>nd</sup> generation of the SiWIM® system [2]. The SiWIM® system is a commercial bridge weigh-in-motion system co-developed by the Slovenian National Building and Civil Engineering Institute and Cestel d.o.o. The system is currently the only B-WIM system capable of calculating dynamic allowance from measurements of the bridge response to the passing vehicles. However, the methods of obtaining the dynamic allowance were, until recently, limited. The most recent development in these methods will be presented in this paper.

An overview of the B-WIM method of measuring traffic loading will be presented, the measure of the dynamic allowance defined and the two methods of obtaining the dynamic allowance described.

The new method will then be described and finally the results obtained from measurements on a bridge will be presented and commented and some examples of dynamic allowance calculations presented.

## 2 Bridge weigh-in-motion and dynamic amplification factor

Bridge weigh-in-motion (B-WIM) systems are applied on existing bridges or culverts from the road network which are transformed into weighing scales [3, 4].

---

<sup>a</sup> Corresponding author: jan.kalin@zag.si

For this purpose the structures are typically instrumented with strain measuring devices. Traditionally, strains are measured on the main longitudinal members of the bridge to provide response records of the structure under the moving vehicle load, but other locations can be used to improve the results. In the case of slab bridges the strain measuring devices are typically mounted at mid-span, across the entire width of the bridge at regular intervals.

Measurements during the entire vehicle passage over the structure provide redundant data, which facilitates evaluation of axle loads. This is an advantage over the pavement WIM systems where an axle measurement lasts only a few milliseconds (with the exception of the multi-sensor installations).

On a large portion of the bridges it is possible to detect individual axles of the passing vehicles using nothing more than sensors mounted underneath the bridge. When that is not possible, additional axle detectors are installed on the pavement.

### 2.1 Theoretical background for B-WIM

The first step in the weighing procedure involves selecting and combining parts of the continuous stream of measured data into so-called events that contain signals from one or more vehicles whose influence on the bridge could possibly overlap. Axles of passing vehicles within events are then identified, their speeds calculated and the individual axles joined into vehicles.

Finally the unknown axle weights  $a_i$  are calculated from a set of equations

$$s(t_j) = \sum a_i I[v_i(t_j - t_i)], \quad (1)$$

where  $s(t_j)$  are the summed values of signals from sensors at different times,  $I(x)$  is the known influence line,  $v_i$  is the axle velocity and  $t_i$  the arrival times of individual axles. The equations can be written in a matrix form  $B\mathbf{a}=\mathbf{s}$ , where the matrix element  $b_{i,j}$  is equal to  $I[v_i(t_j-t_i)]$  and elements of vectors  $\mathbf{a}$  and  $\mathbf{s}$  are simply  $a_i$  and  $s(t_j)$ , respectively. In the current SiWIM® software this over-determined system of equations is solved for  $a_i$  in the least-square sense with the use of the singular value decomposition algorithm [5].

Influence lines, defined as the strain response of the bridge at the sensor location to the passage of a unit axle, are the key structural parameter that is directly related to the quality of B-WIM measurements. The first generation of B-WIM systems used theoretical influence lines, which was sufficient for calculation of relatively accurate gross weights, but it simply could not provide reliable axle loads, especially on shorter spans. Therefore, the latest generations of B-WIM systems always use influence lines that are directly derived from the measured data on the site [6, 7].

Figure 1 presents an example of the result of weighing of a 43.8t five-axle truck passing over an 8m integral concrete slab bridge. The red trace is the sum of measured signals considered in weighing, the black spikes are the positions of the five axles, the green traces

are the influence lines at axle positions, multiplied by raw axle loads and the blue trace is the sum of these axle responses.

Note that the values on the ordinate are measured in volts. The final axle loads are obtained by multiplying the raw values with a calibration factor. This factor is obtained by making a number of passages of a calibration truck with known axle weights and determining the value with which the raw loads must be multiplied to obtain the real loads.

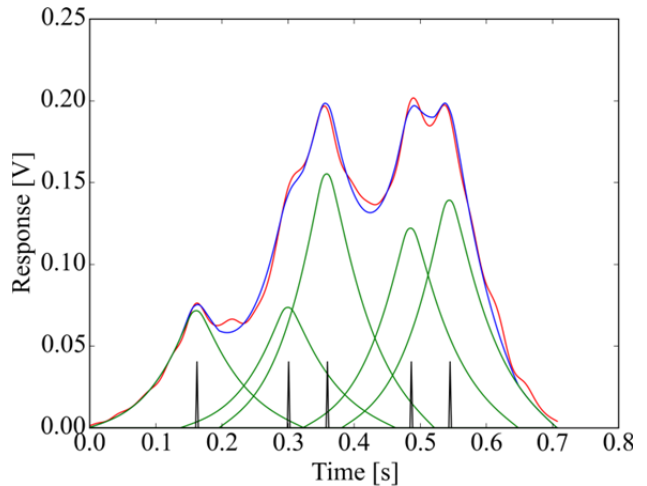


Figure 1. An example of the result of the B-WIM weighing

### 2.2 Dynamic amplification factor

There are several definitions for the dynamic amplification, which can be described as the increase, which occurs in the design load due to presence of dynamic components [1]. In this paper the Dynamic Amplification Factor (DAF) will be defined as  $y_T/y_S$ , where  $y_T$  is the maximum total (static + dynamic) load effect due to a particular loading event and  $y_S$  is the maximum static load effect for the same loading event.

The total load effect is readily available – it is simply the measured response to a vehicle passage. However, the static load effect needs to be estimated from the total load effect. Two methods have, until recently, been used to obtain this estimate.

#### 2.2.1 Sum of calculated axle responses

The first method uses the sum of calculated axle responses, i.e., the blue trace in Figure 1, as the estimated static response. The disadvantage of this method is that a miscalculation of the axle loads can have a large influence on the DAF value. Unfortunately, the likelihood of miscalculation increases precisely in cases where the DAF is likely to be significant – on bridges susceptible to dynamic excitation of traffic.

In Figure 1 the axles in the two tandems are spaced only 1.44m apart, yet the corresponding peaks in the signals are clearly visible. In this case the system of equations (1) is well-conditioned.

On longer bridges, the individual axles are not as easily discernible and the system of equations (1) can

become ill-conditioned. This can be partly mitigated by forcing all axles in a group to have the same load, thereby reducing the number of unknowns in equation (1). However, in the presence of noise, slight miscalculations of vehicle speed and axle spacings and, especially for multiple-presence events, i.e., when a number of vehicles are simultaneously present on the bridge, there is always a chance of erroneous calculation. For example, Figure 2 presents a case where the second axle load of a semi-trailer passing over a 25m beam bridge was calculated to be even slightly negative due to noise (dynamics) in the signal. The system identifies these sorts of numerical problems and flags the vehicles' weights as being incorrect.

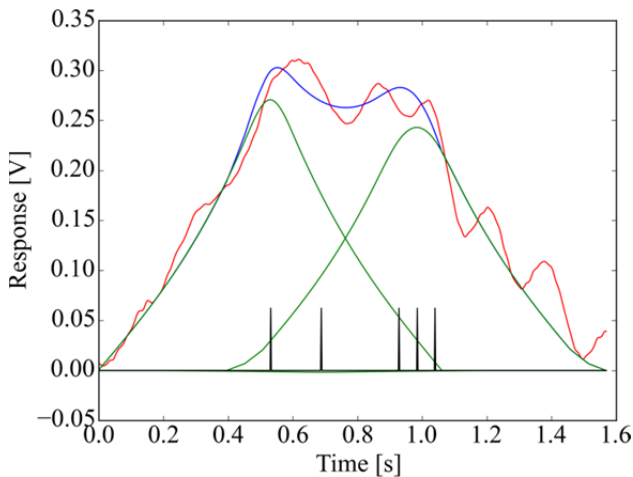


**Figure 2.** An example of miscalculation of axle loads in the presence of noise

Note that the triple axle is represented by a single green trace, since the axles in a group are considered to have the same load and it is the sum of the three appropriately spaced influence lines that is fitted to the measured signal.

In general, axle load miscalculation can have the effect of either overestimating DAF, if the axle near the peak values of the signal is underestimated and, conversely, underestimating DAF if the axle near the peak values is overestimated.

As will be shown later in this paper, when the different methods of evaluating DAF are compared, this can have the effect of distributing DAF values over a wider range and evaluating a significant proportion of them as less than 1.

An additional source of errors is misidentification of axles. Detecting axles, particularly in B-WIMs where this information is obtained from strain measurements underneath the bridge, without using proper axle detectors on the road surface, is generally not a trivial matter. Some types of misidentifications can be corrected; however, there is always a chance that one or more axles are misidentified (missing or added). If this happens to be an axle near the peak value of the signals, the resulting miscalculation of DAF can be quite severe. Two such examples are shown in Figures 3 and 4.

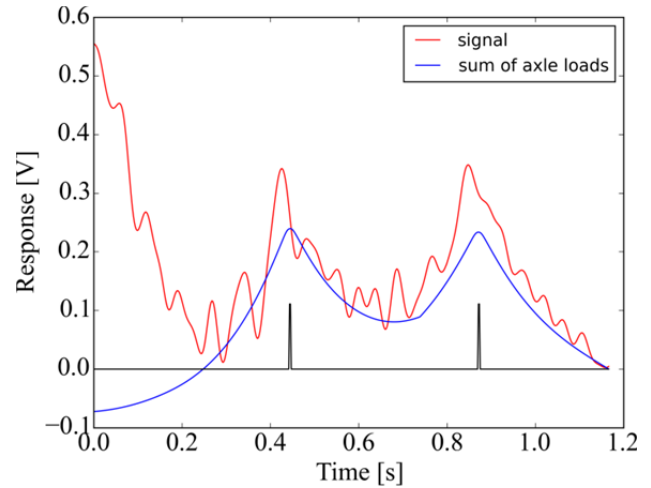


**Figure 3.** Overestimation of DAF

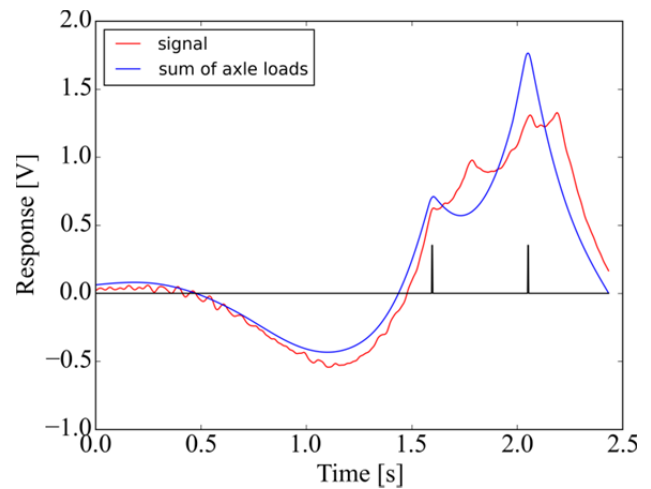


**Figure 4.** Underestimation of DAF

In both events at least one axle was not identified and, as a result, the corresponded axle load could not have been correctly calculated. In the case shown in Figure 3 the static component was grossly underestimated, leading to an unrealistically high DAF value of 2.136.

In Figure 4 four axle peaks are clearly visible in the red trace, but two out of four axles were not identified. The loads of the remaining two axles compensated for the missing axles, resulting in an overestimation of the peak of the estimated static component and an underestimation of DAF, whose value was calculated to be 0.752.

### 2.2.2 Filtering in the frequency domain

The other method assumes that the static and dynamic components of the load effect can be separated based on their characteristic frequencies [1].

The characteristic frequency of the dynamic component is assumed to be higher than the frequencies present in the static component. The signal is transformed into the frequency domain using Fast Fourier Transform [5], the spectrum low-pass filtered at a certain pre-determined cut-off frequency and transformed back into the time domain. Whatever remains is taken as the static load effect and used in the calculation of the DAF value.

The advantage of this method over the previous one is that axle load calculations do not have any effect on the DAF values.

However, certain expertise is required from the user to determine the cut-off frequency. This is performed by looking at a number of signals and, combined with the knowledge of dynamic bridge behaviour, deciding which cut-off frequency would be the best for separation of the components and entering that value into the DAF calculation configuration. If the cut-off frequency is chosen too low, the peaks of the static responses get smeared and the DAF overestimated. If it is too high, the DAF is underestimated, as the approximation to the static response includes some dynamic response.

The method also assumes that there is a clear delineation between the static and dynamic components. In cases of short bridges, where the eigenfrequencies are relatively high, that is a valid assumption. However, for longer bridges a certain region of the spectrum may contain a mixture of the static and dynamic components. In this case a filter other than a simple low-pass filter may be more appropriate. Determining the parameters for such a filter is possibly even more error-prone than determining a simple cut-off value, thus it would be impractical to manually determine the more complex filter parameters.

### 3 The new approach to measuring DAF

Recently a new approach has been developed which tries to combine advantages and overcome disadvantages of both methods.

The aim was to combine insensitivity of the filtering in the frequency domain to axle load calculations with the automatism provided by the axle load calculations. To that end a procedure was devised in which each captured event is processed twice.

#### 3.1 Procedure for obtaining DAF values

In the first phase the axle load calculations are used as a basis to determine the filter parameters. To extend the use to cases where the eigenfrequencies of the bridge could overlap with the spectrum of the axle load response, a piecewise linear function, displayed on Figure 5, was chosen as the filter function.

The filter function is defined by three parameters, the central frequency  $f_0$ , the width  $w$  and the remnant height  $h$ . The remnant height was included in the filter function to possibly pass through a portion of higher frequencies that might be needed to describe the axle load response. Such a filter with  $w=0$  and  $h=0$  corresponds to a low-pass filter. The calculated values  $l=f_0-w$  and  $r=f_0+w$  will be used for easier visualisation of results in section 4.1.

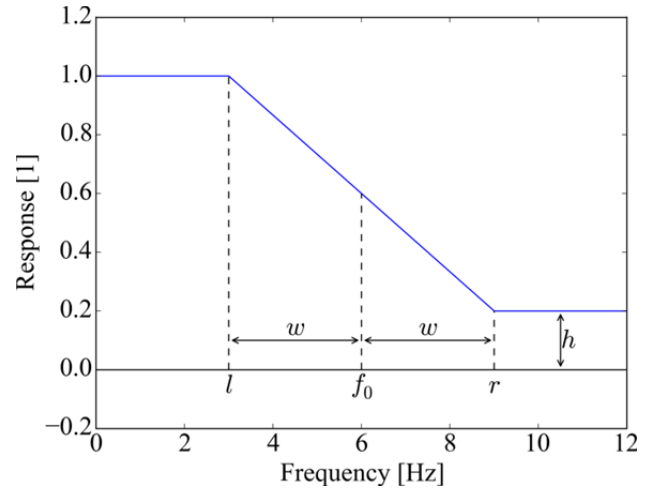


Figure 5. Filter function

A captured event is first evaluated to obtain axle loads. The filter function is then applied to the spectrum of the measured signals and filter parameters adjusted so that the filtered measured signal fits as closely as possible to the curve corresponding to the sum of axle loads. The minimised function is

$$\chi^2(f_0, w, h) = \sum \{s'(t_j | f_0, w, h) - \sum a_i I[v_i(t_i - t_j)]\}^2, \quad (2)$$

where  $s'(t_j | f_0, w, h)$  is the filtered measured response. Powell's method [5] is used to obtain the best-fit values of filter parameters. Since the fitted parameters in the Powell's method are assumed to be real values, but the parameters of the minimised function need to be positive, the absolute values of parameters are taken before evaluating the function.

#### 3.2 Selection of filter parameters for averaging

Because miscalculated axle loads still influence the filter parameters for a specific event, this procedure is repeated for each captured event and the mean values of parameters are chosen as the final filter parameters.

However, not all calculated values are suitable for inclusion in statistics. DAF is not calculated at all if the event contains only cars, so those events were automatically excluded. Additionally, the signal-to-noise ratio is appreciably higher for vehicles with lower axle loads. Considering that the DAF is more significant for vehicles with high axle loads, a gross vehicle weight (GVW) lower limit of 5 tons was adopted for inclusion in the statistics.

Additional errors can sometimes be caused by glitches in the signal. The value of  $\chi^2$ , defined by

$$\chi^2 = \sum \{s(t_j) - \sum a_i I[v_i(t_i - t_j)]\}^2, \quad (3)$$

is calculated during the weighing procedure and used as one of the measures of the quality of results. The typical values vary across different bridges, depending on the length of the bridge, the portion of dynamic component in the signal, the type of traffic, etc

To enable comparison and to obtain some "universal" criterion for judging the quality of results across different

sites, a relative value is used. This is obtained by dividing each value of the  $\chi^2$  by the mean value for that particular site. It has been found during the evaluation of results from a large number of bridges that any relative value above 3 (corresponding roughly to the 95<sup>th</sup> percentile) is a likely sign of a suspicious calculation. The  $\chi^2$  value at the 95<sup>th</sup> percentile was thus chosen as the upper limit for inclusion in the statistics.

Finally, Powell's minimisation method can sometimes stray from the global minimum and get caught in a local minimum. This has the effect of returning nonsensical values of fitted parameters, for example, 1412Hz for the value of  $f_0$ . In order to eliminate these, relatively rare cases, the cases where the  $f_0$  was over 50Hz were discarded.

Once the filter parameters have been obtained, the complete data set is processed again using the frequency domain filtering with the final filter parameters to smooth the measured signal and thus obtain the DAF value for each event.

#### 4 Measuring DAF with the new approach

The first bridge for which this procedure was tested is a highway bridge over the Sava River near Ljubljana, Slovenia. It is composed of seven 20-m long simply-supported spans with a continuous reinforced concrete deck over them. The B-WIM system was installed for 6 months and during that time captured 184266 events. This is not the total volume of traffic passing over the bridge, as the parameters were set to ignore cars. However, in spite of the large number of averaged values, the mean filter parameters were not adequate to satisfactorily filter the signals. In some cases an appreciable portion of the dynamic component remained in the filtered signal.

On further investigation it was determined that the bridge exhibits two distinct vibrational modes, a vertical mode at 9.5Hz and a torsional mode at 15Hz. The two modes are mixed in varying proportions, depending on the excitation, vehicle distribution on the bridge, etc. As a result the obtained mean central frequency obtained with the new procedure falls somewhere between the two natural frequencies and, while the filter adequately suppresses out the torsional vibration, it passes through enough of the vertical vibration to underestimate the DAF in the cases where the vertical vibration is the dominant mode. Further work, which is beyond the scope of this paper, will need to be performed to adequately measure DAF in such circumstances.

A more appropriate bridge with a relatively high dynamic component was chosen. It is an integral frame slab bridge over three spans. The slab thickness is 42cm, the width of the bridge is 7m, the length of the instrumented first span is 7.2m, the length of the central span is 8.9m and the length of the last span is 8.5m.

The short term measurements, lasting for a fortnight, were a part of the regular measurements performed for the Slovenian Road Administration. The vehicle detection was performed with pneumatic sensors, thus in this case also the cars were captured and the total number

of captured vehicles was 19924. Of these, 9800 events contained only cars and were thus not considered, leaving 10124 events that contained trucks (including light vans).

#### 4.1 Filter parameters

The filter parameter calculation procedure was run twice to estimate the influence of the inclusion of the remnant height  $h$  on the minimisation procedure and values. In the first run the remnant height was allowed to be optimised, in the second run it was fixed to 0. After eliminating light vehicles and those whose relative  $\chi^2$  was above the 95<sup>th</sup> percentile, 3989 vehicles were left for the inclusion in statistics. Powell's minimisation failed for the same 14 events in both runs.

The mean values of  $f_0$  and  $w$  for the two runs were within 0.04Hz. The mean and the median values for  $h$ , 0.073 and 0.046 respectively, were quite different and the standard deviation was 0.097. More significantly, the maximum value of  $h$  was 2.3, meaning that in some cases the higher frequencies would have been amplified. This would indicate that, at least in this case, parameter  $h$  should not be included in the optimisation. The results presented in this paper have been obtained with the value of  $h$  fixed to 0. Table 1 lists the values of the filter parameters. All the values are in Hz.

Table 1. Values of filter parameters

Parameter	Mean	Standard Deviation	Median
$f_0$	7.79	1.21	7.96
$w$	0.92	0.42	1.08

Figure 6 shows the distributions of  $f_0$  and  $w$ , overlaid with a Gaussian curve, constructed with their respective means and standard deviations. The distributions are slightly skewed to the left, as the median values are higher than mean values. However, the differences between mean and median values, especially for the relatively small sample size, are negligible.

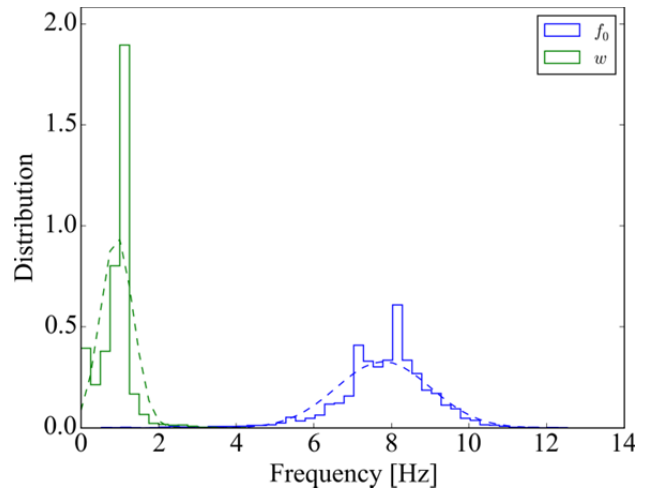


Figure 6. Distributions of  $f_0$  and  $w$

For easier visualisation of the filter function, Figure 7 shows the distributions of  $l$  and  $r$ , the left and right points of the linearly diminishing segment of the filter function, whose mean values are, respectively, 6.87Hz and 8.71Hz.

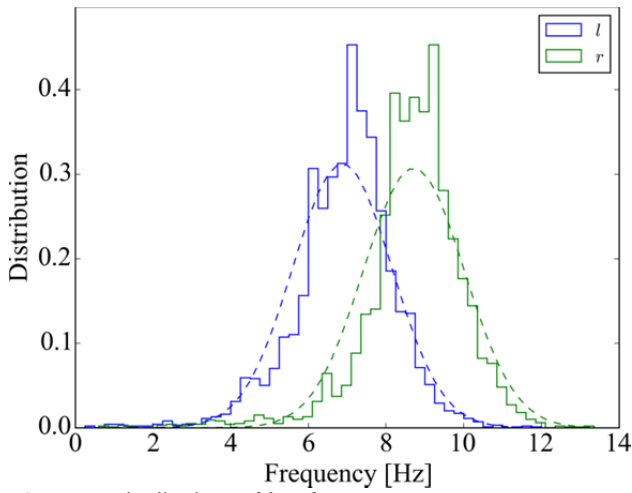


Figure 7. Distributions of  $l$  and  $r$

#### 4.2 DAF measurement

After obtaining the filter parameters, the data set was processed. In the text that follows DAF1 will mean DAF obtained through the use of the sum of axle responses (section 2.2.1), DAF2 obtained by filtering with a simple low-pass filter (section 2.2.2) and DAF3 obtained by the new procedure. For DAF2 the chosen cut-off frequency was chosen to be 7.5Hz.

Table 2 lists the obtained values of DAF, their mean values and standard deviations, maximum and minimum values and the portion of DAF values below 1.

Table 2. Values of DAFs obtained with different methods

DAF	Mean	St.Dev.	Max.	Min.	<1 [%]
DAF1	1.049	0.072	2.316	0.752	16.4
DAF2	1.060	0.042	1.504	0.972	2.6
DAF3	1.046	0.039	1.477	0.965	6.6

The DAF values are similar for all three methods. However, the standard deviation of DAF1 values is significantly higher than the standard deviations of DAF2 and DAF3 values. Correspondingly, the spread of DAF1 values is much larger than DAF2 and DAF2 values.

The portion of values below 1 is also higher for DAF1 values than for DAF2 and DAF3 values. One of the reasons for DAF1 values below 1 has been shown in Figure 4 in section 2.2.1. Another reason, affecting all DAF calculation methods, will be shown in Figure 12 in section 4.4.

Most of the wider spread of the DAF1 values result from the miscalculated axle loadings and the findings indicate the DAF1 method is less suitable for DAF measurements.

Figures 8 through 10 present the dependence of DAF values on the peak measured bridge response within an event, corresponding roughly to the sum of the GVW of vehicles in the event. The larger spread of values of DAF1 can be seen when comparing Figures 8 and 9.

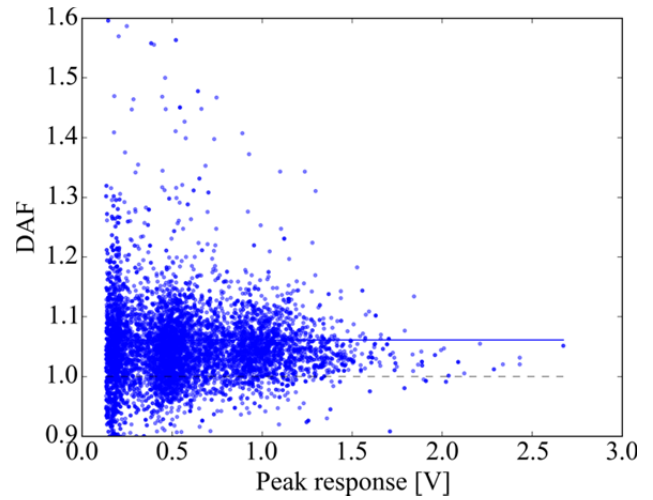


Figure 8. Dependence of DAF1 on peak response

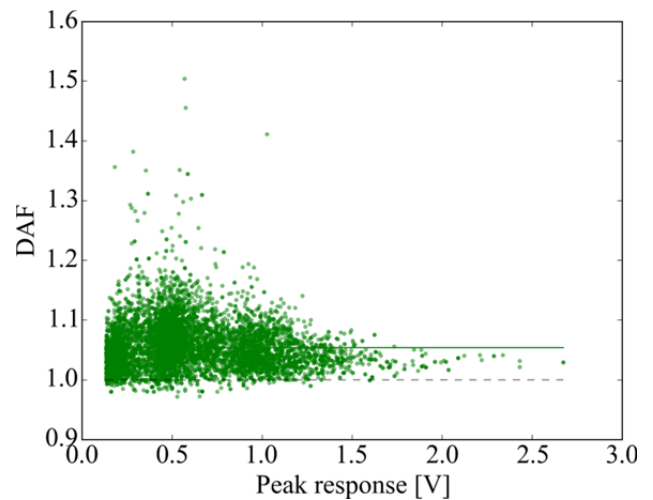


Figure 9. Dependence of DAF2 on peak response

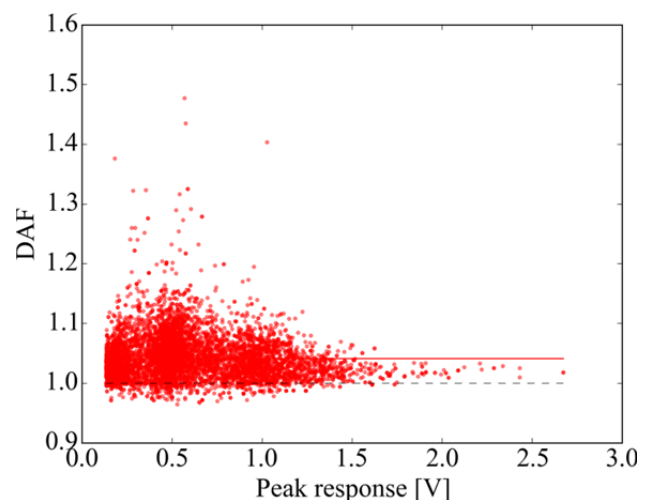


Figure 10. Dependence of DAF3 on peak response

As confirmed by statistics, Figure 9 shows a close resemblance to Figure 10. The mean value of DAF3 is slightly lower than that of DAF2 and a slightly larger portion of DAF3 values are less than 1.

**4.3 Correspondence of DAF2 and DAF3 parameters**

To investigate the correspondence of DAF2 and DAF3 parameters, DAF2 calculations were repeated with cut-off frequencies ranging from 7Hz to 10Hz in steps of 0.5Hz.

For each of the cut-off frequencies the calculation was repeated on the complete set of selected vehicles and the statistics recalculated. The mean DAF2 values are plotted against the cut-off frequency in Figure 11. The dashed line indicates the mean DAF3 value with the DAF3 filter parameters superimposed on it.

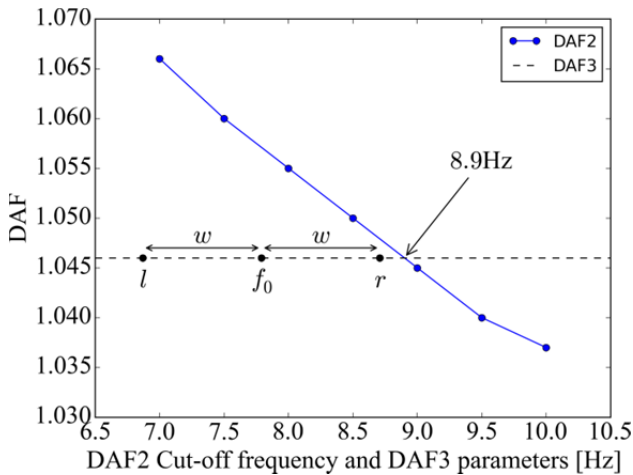


Figure 11. Dependence of mean DAF2 on the cut-off frequency

The graph of the portion of DAF2 and DAF3 values less than 1 (not included in the paper) shows an identical picture — the two lines cross at 8.9Hz. One can say that, in this particular case, the automatically determined filter corresponds to a low-pass filter with a cutoff frequency 8.9Hz, as far as DAF calculations are concerned.

**4.4 Examples**

A few examples of DAF calculations for selected events are presented in this section.

Figure 12 shows the event in which the maximum values for both DAF2 and DAF3 occur, 1.504 and 1.477, respectively.

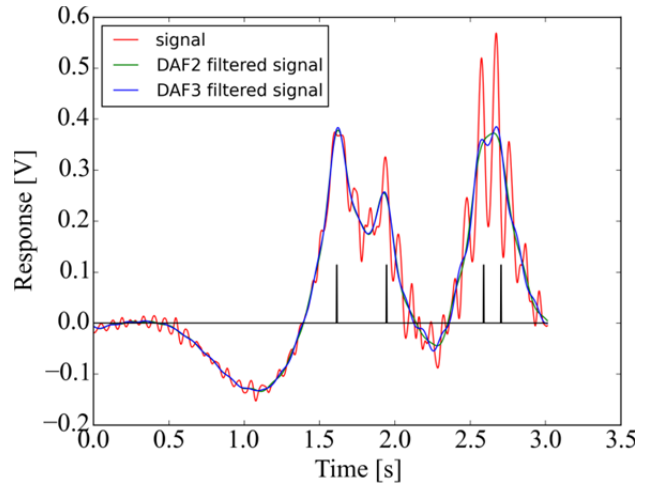


Figure 12. Maximum DAF2 and DAF3 event

This figure also indicates why the DAF3 value tends to be slightly lower than the DAF2 value. The DAF3 filter with the automatically obtained filter parameters admits more of the high-frequency components of the signal into the static component, thus following the signal more closely than the DAF2 filter, causing the ratio of the dynamic-to-static components to decrease.

Figure 13 shows the event with minimum DAF2 and DAF3 values, 0.972 and 0.965, respectively.

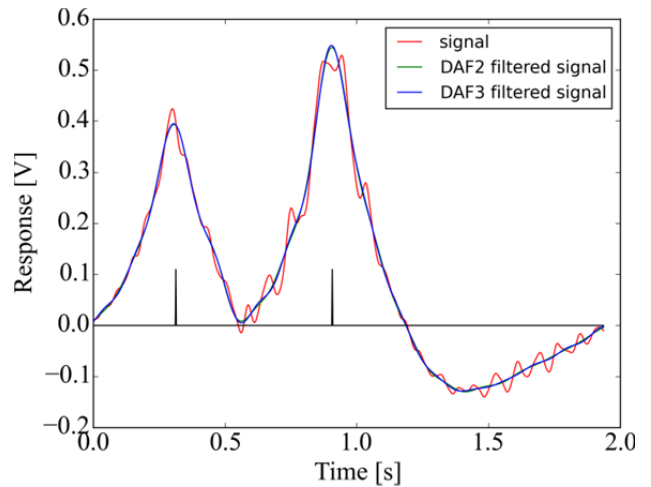
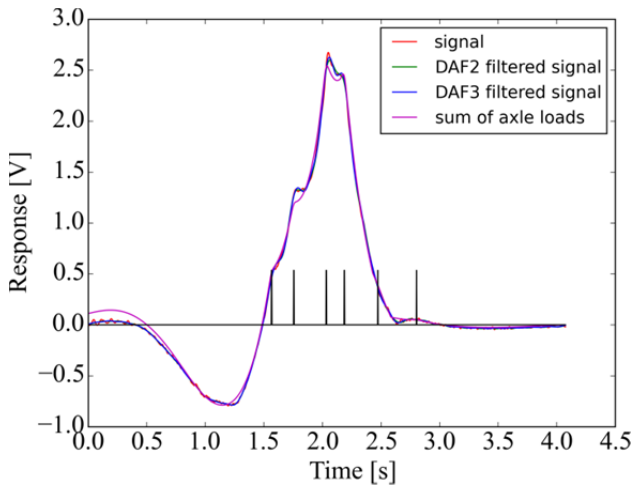


Figure 13. Minimum DAF2 and DAF3 event

In this example the dynamic component of the bridge response just happens to pass through a local minimum at the point of the maximum load. It can thus always be expected that a certain portion of DAF values will be less than 1.

Finally, Figure 14 shows the DAF calculations for the pair of vehicles that induced the highest bridge response (the right-most dot in Figures 8 through 10). The vehicles were a four axle truck with a GVW of 53.6t in one lane (the leftmost four spikes in the black trace) and a car with a GVW of 1.8t in the opposite lane, with the bulk of the response having been caused by the truck.



**Figure 14.** DAF calculations for the vehicle with the highest peak response

The slightly high DAF1 value of 1.051 is caused by a slight error in the calculation of the arrival time of the 3<sup>rd</sup> axle, thus lowering the estimate of the static component. DAF2 and DAF3 values agree with each other, being 1.029 and 1.018, respectively.

More significantly, DAF2 and DAF3 values for the highest peak response event are well below mean values, whereas the maximum DAF2 and DAF3 values were obtained in an event in which the peak response was almost 5 times lower (Figure 12).

#### 4.4 DAF dependence on peak response

These observations are in accordance with those from ARCHES, where it was shown that the DAF decreases for heavier vehicles with more axles.

To investigate the DAF dependence on peak measured signal response, the mean values for all three DAF values were calculated for a subset of events, whose peak responses exceeded some lower limit, ranging from 0.25V to 2.5V in steps of 0.25V.

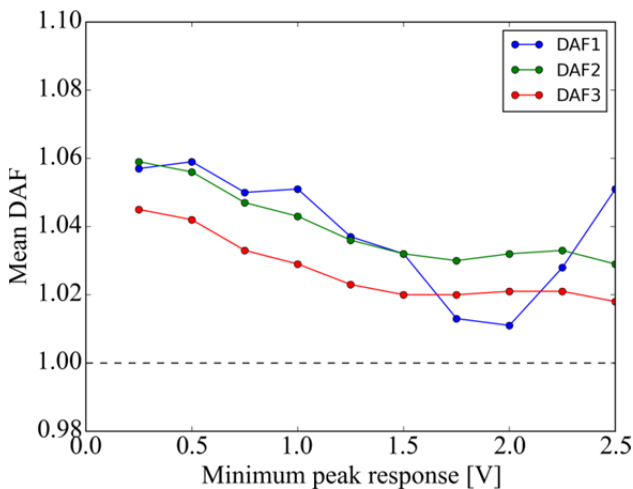


**Figure 15.** Mean values of DAF depending on the minimum peak response for inclusion in statistics

The downward trend is clearly visible in Figure 15 for DAF2 and DAF3. DAF1 displays such a trend in one

region, but the weaknesses of the method again manifest itself at higher minimum peak responses.

## 5 Conclusions

In summary, we can say that the objective, the development of an automated and reliable method for measurement of the DAF, has been met. The proposed method requires almost no intervention from the user and provides good quality DAF values for a slab bridge.

The mean DAF3 value was slightly lower than the mean DAF2 value. As shown in Figure 12, some dynamic component is retained in the estimate of the static component for the calculation DAF3 values, leading to this effect. Perhaps some further narrowing of the selection criteria for inclusion in statistics will need to be considered in the future, which will necessitate processing data from a number of bridges.

Results obtained from this bridge are in accordance with the observations of the ARCHES project, where it was shown that DAF decreases for larger axle loads. Currently the building codes prescribe a relatively large (conservative) dynamic allowance factors. It would thus, in any case, be beneficial to obtain realistic DAF values on as large a number of bridges as possible.

Finally, the method described in the paper has already been implemented in the commercially available SiWIM® B-WIM software and is available for DAF measurements.

## References

1. ARCHES D10: *Recommendations on dynamic amplification allowance*, Brussels: European Commission, <http://arches.fehrl.org/>, (2009)
2. J. Kalin, SiWIM-E®, <http://www.cestel.eu/>, (2015)
3. F. Moses, ASCE J Transp Engrg, **105(3)**, 233-249, (1979)
4. R. Corbally, A. Žnidarič, D. Cantero, D. Hajjalizadeh, J. Kalin, M. Kreslin, C. Leahy, E. J. OBrien, E. Zupan, *Algorithms for Improved Accuracy of Static Bridge-WIM Systems, D3.1 Report of Bridgemon project*, Cestel (2014)
5. W. H. Press, S. A. Teukolsky, W. T. Vetterling, B. P. Flannery, *Numerical Recipes: The Art of Scientific Computing, 3rd. ed.*, Cambridge University Press, (2007)
6. A. Žnidarič, I. Lavrič, *IABMAS2010*, 993, (2010)
7. A. Žnidarič, I. Lavrič, J. Kalin, *IABMAS2010*, 1001 (2010)